Oncogene (2001) 20, 1128–1134
© 2001 Nature Publishing Group All rights reserved 0950–9232/01 $15.00
www.nature.com/onc

Towards a blueprint of the cell cycle

Lilia Alberghina*,[1], Danilo Porro[1] and Lorenzo Cazzador[2]

[1]*Department of Biotechnology and Biosciences, University of Milano-Bicocca, P.zza della Scienza 2, 20126 Milano, Italy;* [2]*Institute of Systems Science and Biomedical Engineering, National Research Council, C.so Stati Uniti 4, 35127 Padova, Italy*

The understanding of the organisation of cell cycle events is of utmost importance to devise effective therapeutic strategies for cancer. In this article we gather evidences from the literature in support of a system model of the cell cycle, in which a growth-sensitive threshold controls entry into S phase and the sequential activation of cyclin-dependent kinases. The cycle is terminated by an End function, that comprises events from the onset of mitosis to cell division and that may also be modulated by the increase of cell size. This blueprint allows quantitative predictions by computer simulations of steady and transitory states. In fact, we show that the proposed control system applies to budding yeast populations during nutritional shift-up and following hyperactivation of the cAMP signalling pathway. Besides the growth-sensitive control system it is shown to apply to mammalian cells both in the exit from quiescence and in active proliferation. The putative molecular determinants that set the threshold controlling S phase entry are consistently altered in cancer cells. Finally, we discuss an input/output analysis based on the simulated behaviour derived from the blueprint as a new tool to investigate the road to cancer. *Oncogene* (2001) **20,** 1128–1134.

Keywords: cell cycle; CDK; CKI; cyclin; budding yeast; cancer

Introduction

Nowadays it is urgently felt the need to describe integrated biological processes such as cell cycle or signal transduction in quantitative functional terms (Hartwell *et al*., 1999). To do so a complex process should be disassembled into basic 'operating units' or 'modules', sub-systems of interacting molecules (proteins, DNA, RNA and smaller molecules) that perform a given function in a way largely independent from the context (Hartwell *et al*., 1999). General design principles, derived from synthetic sciences and engineering, govern the interactions and the function of modules (i.e. switch, threshold control, positive and negative feedback, amplification, robustness, error correction; Hartwell *et al*., 1999). It is interesting to point out that, for a system analysis it is not necessary to know all the components of a module. Instead, the complete knowledge of a module's components is required if one wants to approach the problem following chemical kinetics (Palsson, 1997). A given process could then be described by its blueprint, that is a plan in which its basic modules and governing interactions are identified. The availability of such a blueprint will allow modeling programs to develop to simulate how changes in the module structure or interactions would affect the behaviour of the system. The predictions could then be validated by comparing them with experimental data. In this way and also utilizing findings from genome-wide gene and protein expression analyses, it should be possible to refine the description of the blueprint down to the molecular level.

The purpose of this article is to identify the basic modules of the cell cycle and the design principles linking them. The derived cell cycle blueprint has been tested by computer simulations to predict physiological behaviours both in budding yeast and in mammalian cells and validated by comparing them with experimental findings.

Results

Identification of modules for a cell cycle blueprint

The consistent trend of evolutionary conservation of gene products engaged in the control of the cell cycle from lower eukaryotes to mammalian cells (Hutchison and Glover, 1995 for a review) suggests that the organization of the cell cycle is significantly conserved during evolution and has fostered the role for *Saccharomyces cerevisiae* as a model system.

In *S. cerevisiae*, the basic control system is given by the coordination between increase of the cell size, mostly given by the accumulation of proteins and RNA, and the execution of discontinuous events of the nuclear division cycle, whose more significant steps are DNA replication, chromosome condensation, segregation, and cell division (Johnston *et al*., 1977). A large wealth of information indicates that a critical cell size has to be achieved to enter into the S phase (for a recent review see Futcher, 1996). Several mechanisms have been proposed for the detection of the critical cell size: dilution of an inhibitor (Sompayrac and Maaloe, 1973), building up of an activator (Cooper, 1979) and titration of an inhibitor by an activator (Alberghina *et*

*Correspondence: L Alberghina
Received 23 October 2000; revised 7 November 2000; accepted 16 January 2001

al., 1983). This coordination mechanism determines the specific cell size, protein and DNA contents of cell populations growing at different rates (Tyson *et al*., 1979; Vanoni *et al*., 1983; Alberghina and Porro, 1993).

The commitment to DNA replication and budding occurs in late G1 in an area called Start. The cyclin-dependent kinase (Cdk) encoded by *CDC*28 and associated with the Cln3 cyclin, is the most upstream activator of Start (Tyers *et al*., 1993). While the Cdk abundance per unit of cell protein is roughly constant throughout the cycle (Nasmyth, 1993), changes in the availability of Cln3 modulate the duration of the G_1 phase. Cln3, whose localization appears to be nuclear, has been suggested to monitor the increase in cell size (Futcher, 1996). In this respect, it should be recalled that enhanced levels of Far1 protein (a cyclin-dependent kinase inhibitor, Cki) yield larger cell (Oehlen *et al*., 1996) and that Far1 protein inhibits the activity of Cln3–Cdc28 kinase (Jeoung *et al*., 1998). Further work will tell whether a threshold mechanism, involving Cdc28 or Cln3 as activators and Far1 as inhibitor, controls the entry in S phase in budding yeast.

Overcoming a cell size threshold, allows a cell to enter $S+G_2+M$ phases whose order and timing are set by the sequential activation of a family of Ser/Thr kinases, the cyclin-dependent kinases, activated by their regulatory subunits, the cyclins (Breeden, 2000). In budding yeast only one 'true' Cdk is present, Cdc28 kinase, which is activated by periodically synthesized cyclins: Cln1, Cln2, Clb5 and Clb6 in late G_1, Clb3 and Clb4 in S and G_2, Clb1 and Clb2 in late G_2 and mitosis (Futcher, 1996; Nasmyth, 1996; Breeden, 2000). As a first approximation, the accumulation of a given type of cyclin, G_1 cyclin, S cyclin or G_2+M cyclin, can be considered as the rate limiting step for the activation of the corresponding cyclin–Cdk complex. Since the accumulation of the different cyclins occurs in waves (Futcher, 1996; Nasmyth, 1996) their behaviours may be simulated by a simplified model given by the sequential interconnection of three subsystems presented as a block-diagram in Figure 1. The synthesis of a given cyclin is sparked by the preceeding cyclin and sustained by an autocatalytic process (Breeden, 2000). The accumulation of the subsequent cyclin has a negative feedback effect on the level of the preceding cyclin by stimulating its proteolysis and/or repressing its expression. The cycle model is then terminated by an End function that comprises events from the onset of mitosis to cell division. Several experimental findings argue in favour of this model structure for the autoregulated cyclin waves. Functional Cln3–Cdk drives the synthesis of Cln1 and Cln2 (Stuart and Wittenberg, 1995), which indirectly allow the expression of Clb cyclins (Futcher, 1996). Mitotic Clb cyclins stimulate their own expression while repressing the expression of *CLN* mRNA (Amon *et al*., 1993). On the other hand, G_2 cyclins are required for the proteolysis of Cln1 and Cln2 cyclins (Blondel and Mann, 1996). Cycle specific events require the previous degradation of a given cyclin, for instance cyclin B destruction is needed for exit from mitosis (Murray, 1995).

The blueprint of the cell cycle reported in Figure 1 is clearly a low-resolution one. To gain more information on its structure it will be tested to account for the complex dynamics of cell budding and division in yeast populations undergoing changes of the critical cell size required to enter S phase and of the rate of traverse of the End function.

Blueprint analysis of perturbed S. cerevisiae *populations*

Availability of nutrients has a key role in controlling cell cycle progression in budding yeast. During a nutritional shift-up a rapid decrease in the percentage of budded cells is observed: cells that were before Start at the moment of the shift delay their entry into the S phase, while cells that were after Start delay their exit from the cycle (Alberghina *et al*., 1998). The observed dynamics have been analysed by a simulation programme, described in the Materials and methods section, which incorporates both the protein level required for budding (Ps) and the duration of the budded phase (Tb). The fittings of the predicted percentage of budded cells and of the predicted cell number per volume unit with the experimental data are quite good (Figure 2).

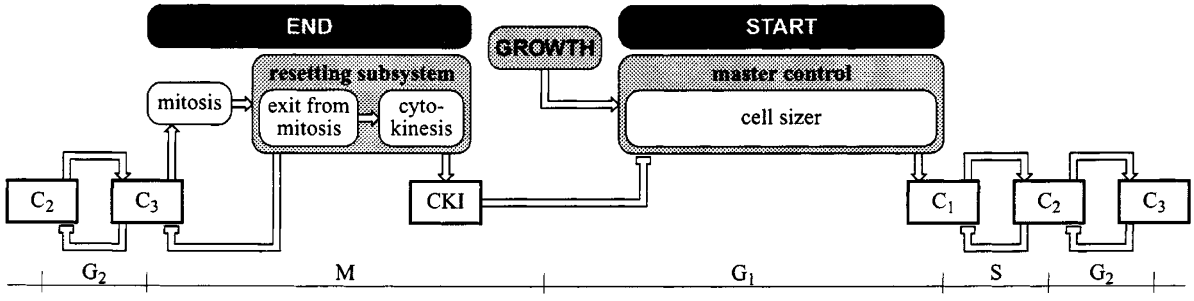

Figure 1 Modelling the sequential interconnections between the main modules of cell cycle progression. The cell cycle blueprint is given by three functional units: a Start function that allows onset of S phase when a critical protein level has been achieved, a cascade of three cyclin subsystems (namely C1, C2, C3) and an End function that comprises the events from onset of mitosis to cell division

Since the addition of glucose increases the level of cAMP in yeast cells (Thevelein, 1991), one may suggest that at least part of the effect of glucose on proliferation and cell cycle progression could be mediated by cAMP, whose requirement for the execution of early events of Start is well established (Broach, 1991). When cAMP is added to growing budding yeast cells, the critical protein content Ps required for budding is increased (Baroni *et al*., 1992) and the expression of *CLN*1 and *CLN*2 cyclins is repressed (Baroni *et al*., 1994). The addition of cAMP brings a sharp decrease in the percentage of budded cells (BI), while the increase in cell number is unaffected for more than 1 h, then it remains constant for about 2 h before it starts to increase again at a rate comparable to that of untreated cultures (Alberghina *et al*., 1998; Baroni *et al*., 1992). The comparison of the experimental growth data and of the percentage of budded cells with the simulation data is as satisfactory as for the shift-up (Figure 3).

From the simulation analysis it is possible to derive the transient evolution of Tb and Ps, estimated from the best fitting of the simulated behaviour to the experimental data (Figures 2b,c and 3b,c). For the shift-up, the estimated Ps, assumed to be equal to 1 in the preexisting cells, increases slowly for about 3.5 h to reach the value detected during proliferation in the richer medium (Ps = 1.7). The duration of the budded phase increases immediately from 2.5 h to 3.3 h, in agreement with the experimental findings (Alberghina *et al*., 1998), then it slowly declines to reach the value characteristic of the new medium (1.4 h) 3.5 h after the shift-up. It has been shown previously that daughter cells standing at Start at the moment of the shift-up have a Tb duration of 3.5 h, while daughter cells born at 45 min or later after the shift have a Tb of 1.4 h (Alberghina *et al*., 1998).

In the hyperactivation of cAMP pathway, Ps starts to increase immediately after cAMP addition and this increase is maintained for the entire observation period. Tb increases from 1.3 h to reach a new apparent steady value of 1.8 h after 4 h. The differences with the pattern observed for the shift up are significant.

In conclusion, the blueprint analysis of perturbed yeast populations has allowed attainment of kinetic evidences on the whole population about the complex relations between proliferation and cell cycle progression. Nutritional shift-up and hyperactivation of the cAMP pathway in growing cells interfere with the Start function bringing a sudden drop in the ability to enter S phase and an increase of Ps that builds up slowly with time. Nitrogen-starved yeast cells pause in G_1 even if they have reached a cell size that allows budding in unstarved cells. Such a response appears to be related to reduced mRNA translation and enhanced protein degradation for Cln3 (Gallego *et al*., 1997). A reduction of the availability of Cln3, due to its degradation or to a nuclear to cytoplasmic delocalization, during the early period of shift-up and of cAMP addition, could force pre-Start cells to delay their entry into S phase.

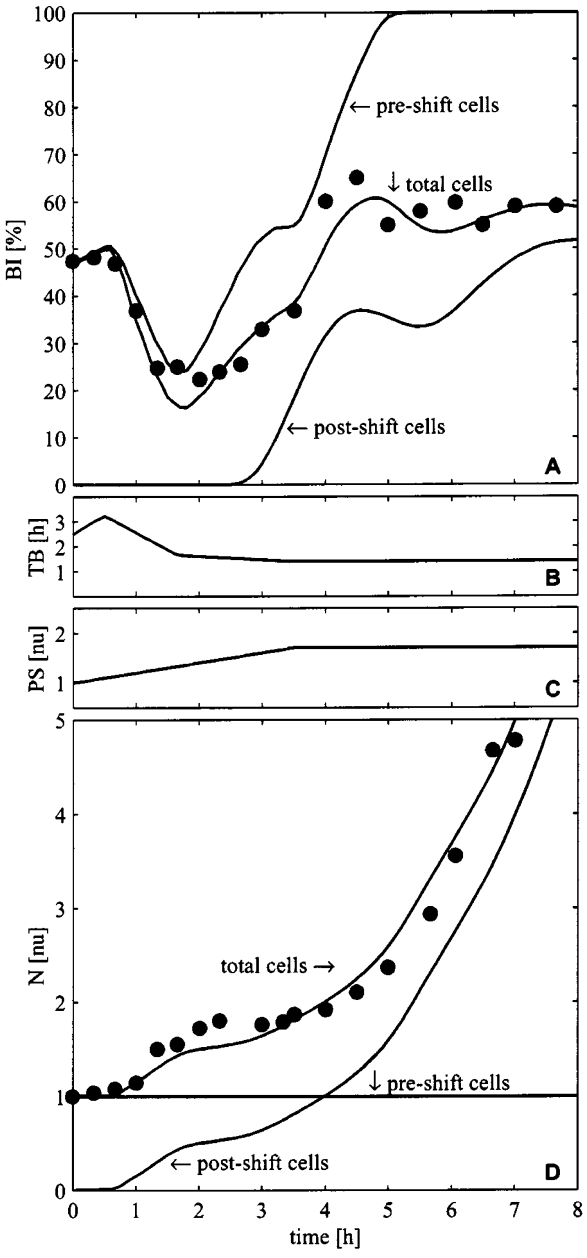

Figure 2 Effects of a nutritional shift-up on the behaviour of the budding index (BI), total number of cells (N), length of the budded phase (T_B) and size at budding (Ps). Comparison between experimental and simulated data (data redrawn from Alberghina *et al*., 1998). S288C yeast cells were grown in ethanol-YNB medium till exponential phase ($\mu = 0.156\ h^{-1}$), washed and resuspended into glucose-YNB medium (T = 0). The specific growth rate of the yeast population during the newly reached balanced growth conditions (T = >4) was $0.327\ h^{-1}$. (**a**) Experimental (●) and simulated (−) percentage of budded cells for the whole population (total cells), for cells born after resuspension into the new growth medium (post-shift cells), as well as for cells born during growth on ethanol (pre-shift cells). (**b**) Estimated time course of the average length of the budded phase (T_B: S + G2 + M; h) of dividing pre-shift cells. (**c**) Estimated time course of the size at budding (Ps) for pre-shift cells (Ps is taken as 1 in cells growing on ethanol). (**d**) Experimental (●) and simulated (−) number of cells for total cells, post-shift cells and pre-shift cells

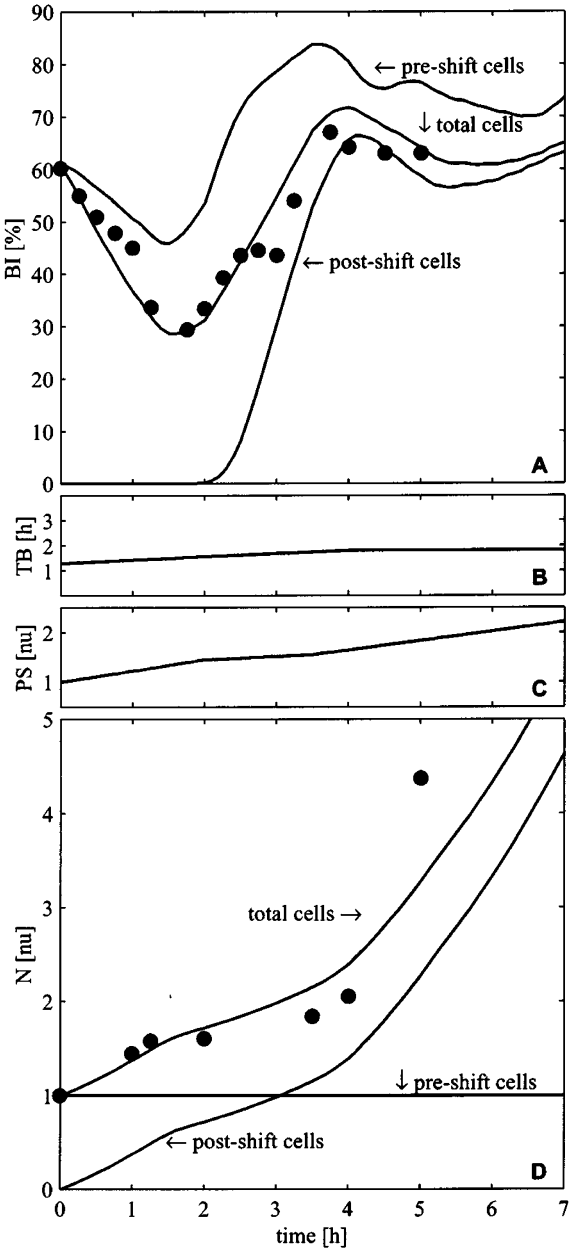

Figure 3 Effects of the addition of cAMP on the behaviours of the budding index (BI), total number of cells (N), length of the budded phase (T_B) and size at budding (Ps). Comparison between experimental and simulated data (data redrawn from Alberghina *et al*., 1998). To cAMP-permeable OL214 yeast cells grown on glucose-YNB medium so to reach the balanced exponential phase ($\mu = 0.370$), cAMP was added at time T = 0 (final concentration: 3 mM). The specific growth rate of the yeast population before and after the addition of cAMP did not change (Alberghina *et al*., 1998; Baroni *et al*., 1992). (**a**) Experimental (●) and simulated (−) percentage of budded cells for the whole population (total cells), for cells born after addition of cAMP (post-shift cells), as well as for pre-shift growing cells. (**b**) Estimated time course of the average length of the budded phase (T_B: S + G2 + M; h) of dividing pre-shift cells. (**c**) Estimated time course of the size at budding (Ps) for pre-shift cells (Ps is taken as 1 in pre-shift growing cells). (**d**) Experimental (●) and simulated (−) number of cells for total cells, post-shift cells and pre-shift cells

As for the End function, a sudden increase of Tb is observed in shifting up cells at the moment of the shift-up (Figure 2b), due to a delay in cell division. An arrest in metaphase or in late anaphase is observed in growth-limited cells after addition of cAMP (Anghileri *et al*., 1999), while Tb (Figure 3b) increases only slightly in growing cells. These findings as well as the reported effects of growth on wee-1 and nim1 activities (Booher *et al*., 1993; Tanaka and Nojima, 1996) indicate that growth and cAMP control the End function at three distinct levels, at the onset of mitosis, at the metaphase/anaphase transition and at the exit of mitosis.

Blueprint analysis of normal and transformed mammalian cells

The model of Figure 1 appears to account also for the basic regulatory circuits of the cell cycle in mammalian cells, as indicated by the following data.

In mammalian fibroblasts the accumulation of active cyclin D-Cdk4 as well as of active cyclin E-Cdk2 is required in late G_1 phase to activate the transcriptional program that promotes passage to S phase (Sherr, 1994). The levels of the Cki $p21^{Cip1}$, $p27^{Kip1}$, $p16^{INK4a}$ and $p15^{INK4b}$ are taken to set a threshold that determines the timing of expression of active G_1 cyclin dependent kinases (as reviewed from Perez-Roge *et al*., 1999). Growth factors, antimitogens, contact inhibition, DNA damage, and senescence may largely modulate the levels of Cki (as reviewed from O'Connor, 1997). Figure 4 illustrates a putative threshold control over the entrance into S phase in mammalian cells. It states that Cdk4 and cyclin D act as activators and $p21^{Cip1}$, $p27^{Kip1}$, $p16^{INK4a}$ and $p15^{INK4b}$ as inhibitors of the threshold mechanism taken to coordinate proliferation and cell cycle progression (Alberghina *et al*., 1983). The threshold mechanism of Figure 4 can be integrated with the cell cycle model of Figure 1, so to allow to link the dynamics of cyclin D accumulation with the timing of cell cycle progression.

One of the questions that have puzzled investigators for a long time is why the addition of mitogens to quiescent G_0 cells is followed by entry in S phase after 10–12 h, while in cycling cells the duration of the G_1 phase is about 5 h (Baserga, 1976). Since it has been observed that the cyclin D is undetectable in quiescent cells (Won *et al*., 1992), and that overexpression of D-type cyclins shortens G_1 phase in mouse fibroblasts (Quelle *et al*., 1993), a simulation analysis has been performed to examine the link between growth-dependent synthesis of cyclin D and the timing of the onset of S phase in cells recovering from quiescence.

The addition of serum to quiescent fibroblasts, that have a smaller cell size than cycling cells (Alberghina, 1977) and undetectable levels of cyclin D (Won *et al*., 1992), stimulates growth at a rate of $0.049\ h^{-1}$ corresponding to a duplication time of 15 h (Zetterberg and Layson, 1995). The simulation shown in Figure 5a has been performed assuming a first order kinetics for the accumulation of cyclin D, and setting the amount

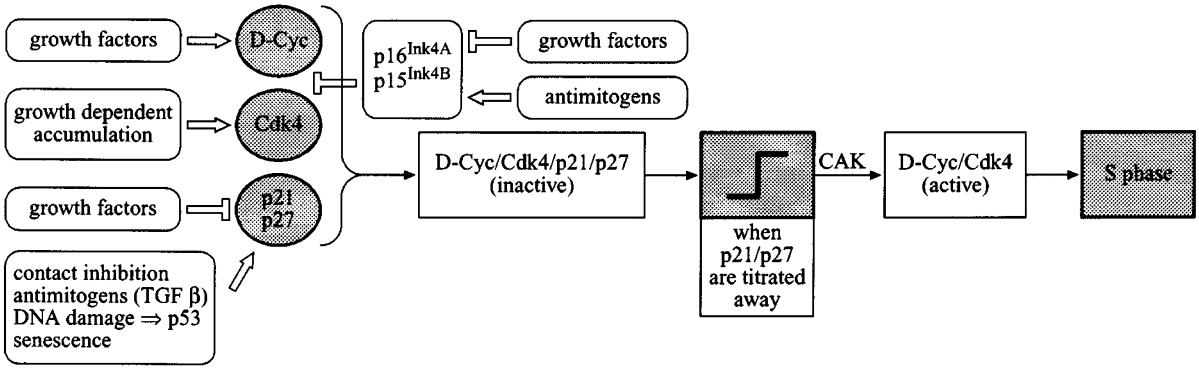

Figure 4 The putative threshold controlling the entrance into the S phase in mammalian cells. Cdk4 and cyclin D act as activators and $p21^{Cip1}$, $p27^{Kip1}$, $p16^{INK4a}$ and $p15^{INK4b}$ as inhibitors of the threshold mechanism. Increase in cell size is monitored by the constant level of cyclin D. In cycling cells, the amount of cyclin D-Cdk4 is proportional to cell mass and CyclinD-Cdk4 interacts with the various Cki forming inactive complex. When all the present Cki have been titrated away, active cyclin D dependent kinase is formed and the activation of the transcriptional programme that bring to S phase takes place

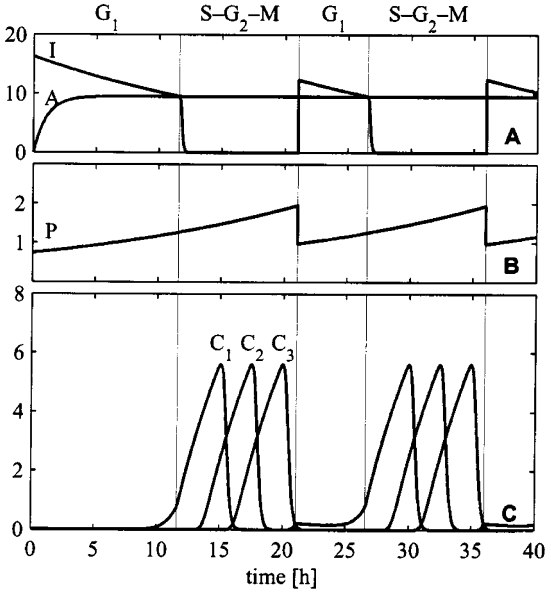

Figure 5 Simulation of the transition from quiescence to proliferation in mammalian cells. Growth stimulation of quiescent cells induces the accumulation of total proteins P and the synthesis of the activator A, cyclin D whose level is undetectable in quiescent cells. Entry into S phase occurs when the inhibitor Cki, taken to be a fixed amount at division, is titrated away by the activator. This event is followed by a degradation of the inhibitor, which allows the triggering of a cascade of cyclins (namely C_1, C_2, and C_3) up to cell division, when the initial level of inhibitor is restored. Newborn cycling cells are larger than quiescent cells and are endowed of a level of activator (cyclin D) characteristic of proliferating cells, therefore they move into the S phase after a shorter G_1 period than the quiescent cells, while cross $S+G_2+M$ phase in the same time. (**a**) Concentration of activator A and inhibitor I in arbitrary units; (**b**) Amount of total proteins normalized to the level at birth in steady state taken as 1. (**c**) Concentrations of cyclins in arbitrary units

of inhibitor Cki in such a way that 11.2 h are needed to reach the cyclin D concentration required to titrate all Cki and therefore to overcome the Ps threshold (Figure 5b). The waves of S and G_2+M cyclins develop in the following 9.4 h. The following symmetrical cell division endows the daughter cells with amounts of cyclin D, of Cki and with a cell size that in cycling cells sets the duration of the G_1 phase to 5.6 h and the length of the duplication time to 15 h (Figure 5c), all in close agreement with experimental findings. This simulation indicates that there is a congruity, in the frame of the model presented in Figure 1, between levels and dynamics of accumulation of cyclin D and cell mass on one hand and the timing of G1 phase and cell cycle duration on the other, both in the recovery from quiescence and in cycling cells.

An additional observation can be derived from the model of Figure 1 in relation to cancer cells. It is quite well known that overexpression of cyclin D (Motokura and Arnold, 1993), mutations of Cdk4 that reduce its ability to be inhibited by Cki (Wolfel *et al*., 1995), decreased levels, mutations, deletions or increased degradation of $p21^{Cip1}$ and of $p27^{Kip1}$, mutations or deletions of $p15^{INK4b}$ and $p16^{INKa}$ (Hunter and Pines, 1994), mutations or deletions of p53 (Kastan *et al*., 1995) take place in cancer cells. Considered in the frame of the threshold model of the cell cycle discussed in this paper, all these molecular alterations converge to change the setting of the threshold controlling the entry in S phase, facilitating its overcoming. The coordination between growth and cell cycle progression will then be altered with a tendency to yield smaller cells. This event could put a significant selective constrain on the clonal evolution of transformed cells.

Discussion

The blueprint of the cell cycle discussed in this article could offer a framework in which to embed a large number of experimental findings on cell cycle regulation both in budding yeast and in mammalian cells. Its main regulating event is a Start function, in which a 'cell sizer' controls entry into S phase, by activating waves of cyclins that set the timing of the onset of mitosis and of cell division.

Growth modulates several rate limiting steps both for the entry into S phase and for the execution of mitosis. Computer simulation analyses based on this blueprint allowed to put into a quantitative relation the changes in the values of one or more of the rate-limiting steps with phenomenological properties of cell proliferation measured either as growth rate or as percentage of budded cells in yeast. It is an easy prediction that they will also do so with DNA and protein distributions obtained by flow cytometry. It is therefore feasible to perform quantitative input/output analysis in which putative molecular determinants of the rate-limiting steps are modified either by genetic or by metabolic means and the behaviour of cell proliferation will be analysed both experimentally and by simulation. The results of such an analysis will be useful in identifying the molecular determinants of the rate-limiting steps. By complementing this new approach with the more classical analysis of cell cycle regulation such as genetic interactions (for instance synthetic lethality), genome-wide gene and protein expression and analysis of interacting proteins, it should be possible to move from the actual sketchy blueprint to one defined at the molecular level. As a consequence, it is likely that this approach will also offer a useful tool to investigate the road to cancer.

Materials and methods

Modelling cell population dynamics

The simulation of growth and proliferation of a budding yeast culture (see Figures 2 and 3) has been developed from the population model described by Mariani *et al*. (1986). In that formulation, the cell cycle is fully described by a simplified deterministic model based on: the specific growth rate μ, at which cell size (or protein content) increases; the critical size Ps, at which unbudded cells start budding; the size Pd, at which cell division is completed. Although Ps and Pd slightly increase at each new generation (Hartwell and Unger, 1977), the present analysis assumes, to simplify and speed up the simulations, that they are independent from the genealogical age, without remarkably affecting the predicted behaviour.

From the cell cycle model a population model has been developed, describing the time evolution of the density distribution function f(x,t). This function represents the state of the population with reference to its distribution along all the possible cell sizes: f(x,t) dx gives the number of cells having size between x and x + dx at time t. The simulation program performs two main tasks: to predict the time evolution of f(x,t) starting from a given initial value to deal with varying culture conditions. Three parameters influence the simulated dynamics: μ, Ps and Pd.

To perform a more reliable and realistic analysis, the cell cycle model has been modified to account for cell growth variability around the mean value μ. The produced effect can be summarized as follows: a given cohort of cells, all with the same size, spreads, during growth, around a mean value, corresponding to that of the deterministic case, and with variance increasing with the size increase.

The relationship between Ps and Pd can be represented either with reference to the relative size increase, i.e., the adimensional parameter h = Pd/Ps, or to the duration of the budded phase, i.e., the parameter Tb. While h is a well defined deterministic parameter, because Ps and Pd are assumed to be deterministic, Tb is not, because it depends on the growth rate. The mean Tb value has been estimated from the value predicted by the fully deterministic model, i.e., from the solution of equation:

$$\mathrm{Ps(t\text{-}Tb)}\ \exp\left\{\int_{\mathrm{t\text{-}Tb}}^{\mathrm{t}} \mu(z)\mathrm{d}z\right\} = \mathrm{Pd(t)} \qquad (1)$$

In fact, a cell divides at time t after a period Tb only if there is a size increase from Ps, at time t-Tb, to Pd, at time t; the exponential function represents the relative size increase.

The setting of cell size threshold (Ps) controlling the entry into S phase has been taken to depend on the interactions between inhibitors and activators of protein kinase Cdk. The essential features of this mechanism were proposed and modelled by Alberghina *et al*. (1983). In stationary conditions, the amount of inhibitor I endowed to a cell is constant at birth; the intracellular concentration of activator A is constant so that the total amount of A is proportional to the cell size. The critical size for entry in S phase (Ps) is achieved when the endowed inhibitor is completely titrated by the activator.

Modelling cyclin dynamics (Figure 5)

To investigate the functional properties of the interactions between size control mechanism and the activation of waves of cyclins, a functional model has been developed. It assumes that three cyclin dependent components, C_1, C_2 and C_3 are required for the following transitions: C_1 for G_1 to S; C_2 for S to G_2; C_3 for G_2 to M.

The mass balance equation for each cyclin component has the following general form:

$$\mathrm{d[C]/dt} = \mathrm{m\,p} \quad (\mathrm{d} + \mu)[\mathrm{C}] \qquad (2)$$

where [C] represents the intracellular concentration, p and d the rates of synthesis and degradation, μ the specific cellular growth rate, and m a function modulating the synthesis. Rates p and d have been empirically chosen to reproduce: synthesis activation through $[C_{-1}]$, the concentration of the previous component; synthesis amplification by a positive feedback on [C]; degradation activation through $[C_{+1}]$, the concentration of the next component. Function m is equal to 1 for C_2, and C_3, while for C_{-1} it varies from 0 (when [A] < [I]) to 1 (when [A] > [I]), with a smooth transition.

Figure 5 shows a typical evolution: after cell division (at $t = 0$), C_1 is activated when I is titrated away by A; the sharpness or smoothness of the transition around [I] = [A] depends on the shape of m. The cascade of waves of cyclins is given by the forward activation of C_2 and C_3, together with the backward degradation of C_1 and C_2.

References

Alberghina L. (1977). *J. Theor. Biol.,* **69,** 633–643.
Alberghina L, Martegani E, Mariani L and Bortolan G. (1983). *BioSystems,* **16,** 297–305.
Alberghina L and Porro D. (1993). *Yeast,* **9,** 815–823.
Alberghina L, Smeraldi C, Ranzi BM and Porro D. (1998). *J. Bacteriol.,* **180,** 3864–3872.
Amon A, Tyers M, Futcher B and Nasmyth K. (1993). *Cell,* **74,** 993–1007.
Anghileri P, Branduardi P, Sternieri F, Monti P, Visentin R, Bevilacqua A, Alberghina L, Martegani E and Baroni MD. (1999). *Exp. Cell Res.,* **250,** 510–523.
Baroni MD, Monti P and Alberghina L. (1994). *Nature,* **371,** 339–342.
Baroni MD, Monti P, Marconi G and Alberghina L. (1992). *Exp. Cell Res.,* **201,** 299–306.
Baserga R. (1976). *Multiplication and division in mammalian cells.* Marcel Dekker (ed)., New York.
Blondel M and Mann C. (1996). *Nature,* **384,** 279–282.
Booher RN, Deshaies RJ and Kirschner MW. (1993). *EMBO J.,* **12,** 3417–3426.
Breeden LL. (2000). *Curr. Biol.,* **10:** R586–R588.
Broach JR. (1991). *Trends Genet.,* **7,** 28–33.
Cooper S. (1979). *Nature,* **280,** 17–19.
Futcher B. (1996). *Yeast,* **12,** 1635–1646.
Gallego C, Gari E, Colomina N, Herrero E and Aldea M. (1997). *EMBO J.,* **16,** 7196–7206.
Hartwell LH, Hopfield JJ, Leibler S and Murray AW. (1999). *Nature,* **402**(Suppl.): C47–C52.
Hartwell LH and Unger MV. (1977). *J. Cell. Biol.,* **75,** 422–435.
Hunter T and Pines J. (1994). *Cell,* **79,** 573–582.
Hutchison C and Glover DM (ed). (1995). *Cell Cycle Control.* IRL Press at Oxford University Press.
Kastan MB, Canman CE and Leonard CJ. (1995). *Cancer Met. Rev.,* **14,** 3–15.
Jeoung D, Oehlen LJWM and Cross FR. (1998). *Mol. Cell. Biol.,* **18,** 433–441.
Johnston GC, Pringle JR and Hartwell LH. (1977). *Exp. Cell. Res.,* **105,** 79–98.
Mariani L, Martegani E and Alberghina L. (1986). *IEE Proceedings Pt. D,* **vol. 133,** 210–215.
Motokura T and Arnold A. (1993). *Curr. Opin. Gen. Dev.,* **3,** 5–10.
Murray A. (1995). *Cell,* **81,** 149–152.
Nasmyth K. (1993). *Curr. Opin. Cell Biol.,* **5,** 166–179.
Nasmyth K. (1996). *Trends Genet.,* **12,** 405–412.
O'Connor PM. (1997). *Cancer Surv.,* **29,** 151–182.
Oehlen LJ, McKinney JD and Cross FR. (1996). *Mol. Cell. Biol.,* **16,** 2830–2837.
Palsson BO. (1997). *Nature Biotechnol.,* **15,** 3–4.
Perez-Roge I, Kim S-H, Griffiths B, Sewing A and Land H. (1999). *EMBO J.,* **18,** 5310–5320.
Quelle DE, Ashmun RA, Shurtleff SA, Kato JY, Bar-Sagi D, Roussel MF and Sherr CJ. (1993). *Genes Dev.,* **7,** 1559–1571.
Sherr CJ. (1994). *Cell,* **79,** 551–555.
Sompayrac L and Maaloe O. (1973). *Nature,* **241,** 133–135.
Stuart D and Wittenberg C. (1995). *Genes Dev.,* **9,** 2780–2794.
Tanaka S and Nojima H. (1996). *Genes Cells,* **1,** 905–921.
Thevelein JM. (1991). *Mol. Microbiol.,* **5,** 1301–1307.
Tyers M, Tokiwa G and Futcher B. (1993). *EMBO J.,* **12,** 1955–1968.
Tyson CB, Lord PG and Wheals AE. (1979). *J. Bacteriol.,* **138,** 92–98.
Vanoni M, Vai M, Popolo L and Alberghina L. (1983). *J. Bacteriol.,* **156,** 1282–1291.
Wolfel T, Hauer M, Schneider J, Serrano M, Wolfel C, Klehmann-Hieb E, De Plaen E, Hankeln T, Meyer zum Buschenfelde KH and Beach D. (1995). *Science,* **269,** 1281–1284.
Won KA, Xiong Y, Beach D and Gilman MZ. (1992). *Proc. Natl. Acad. Sci. USA,* **89,** 9910–9914.
Zetterberg A and Layson O. (1995). In *Cell Cycle Control.* Hutchison C and Glover DM (ed)., IRL Press at Oxford University Press.